Available online at www.sciencedirect.com
ScienceDirect
Journal of the European Ceramic Society 29 (2009) 1763–1770
www.elsevier.com/locate/jeurceramsoc

Chemical and thermomechanical compatibility between neodymium manganites and electrolytes based on ceria

V. Gil, J. Tartaj, C. Moure *

Instituto de Cerámica y Vidrio (CSIC), Electroceramics Department C/ Kelsen 5, 28049 Madrid, Spain

Received 29 August 2008; accepted 17 October 2008
Available online 28 November 2008

Abstract

The goal of this work was to study the thermal expansion behaviour of $NdMe_{0.5}Mn_{0.5}O_3$ (Me = Ni, Co) solid solutions and to establish the phase relations between them, used as cathodes, and two electrolytes based on $Ce_{0.9}Gd_{0.1}O_{1.95}$. The electrolyte was doped with 1.0 wt% Bi_2O_3 in order to improve the final densification.

Intimate mixtures of the cathode and electrolyte powders were reacted at several temperatures for studying the possible reaction products. Cathode–electrolyte pairs were obtained by isostatic pressing of constituent powders and subsequent sintering in the temperature range 1350–1400 °C for 2 h to observe the interphase compatibility. The sintering conditions were optimized to obtain highly densified electrolytes and well-developed cathode–electrolyte interfaces. Scanning electron microscopy observation with EDAX analysis was performed in cathode–electrolyte interfacial regions in order to characterize the obtained microstructures and to determine possible cation interdiffusion between the cathode and the electrolyte.

The nickel-doped manganite, $NdNi_{0.5}Mn_{0.5}O_3$, is chemically and thermo-mechanically compatible with both electrolytes without formation of new phases up to 1400 °C even during long treatment times. On the other hand, $NdCo_{0.5}Mn_{0.5}O_3$ perovskite not had a good behaviour with none of the electrolytes.

Keywords: Powders-solid state reaction; Interfaces; CeO_2; Fuel cells

1. Introduction

In the last decades, lanthanum manganites have been widely investigated [1–3] as electrodes for SOFC cathode applications, specifically those modified with alkaline earth cations, due to their good electrical conductivity and relatively low cost. Nevertheless, they present problems due to lanthanum reaction at high temperatures with YSZ electrolytes [4–6] forming secondary, isolating phases such as $La_2Zr_2O_7$. Furthermore, alkaline earth cations employed can also react with zirconia or with ceria-based electrolytes, forming perovskite-type zirconates ($SrZrO_3$) and Ba, Sr cerates, respectively. These secondary phases can cause poor conductivity or even form insulating interfaces. In order to overcome these problems, it is necessary to employ new materials for SOFC cathodes operating at intermediate temperature. The materials proposed are manganites, in which lanthanum is replaced by a rare earth with lower ionic-radius cation such as neodymium and, in which Mn has been partially replaced by a divalent cation on the B sites (transition metals such as Me = Ni, Co), $NdMe_{0.5}Mn_{0.5}O_3$. The substitutions in the perovskite structure of lanthanum by neodymium on the A sites and of transition metals on the B sites are proposed as an alternative to obtain chemically more stable systems.[7] The possible pyrochlore phase formation from heavy rare earth cations possess a lower stability at sintering and operating temperatures and the reaction with electrolytes based on ceria should be less likely to take place.

For successful long-term operation of SOFCs, a good compatibility among the ceramic materials is crucial. Therefore, cation diffusion and reaction within the cathode/electrolyte interface should be avoided.

Ceria-based electrolytes, having a higher ionic conductivity than YSZ work at lower temperatures between 600 and 800 °C. The present paper establishes the phase relations between two electrolytes based on $Ce_{0.9}Gd_{0.1}O_{1.95}$ ceramics and $NdMe_{0.5}Mn_{0.5}O_3$ (Me = Ni, Co) solid solutions acting as

* Corresponding author.
E-mail address: cmoure@icv.csic.es (C. Moure).

0955-2219/$ – see front matter © 2008 Elsevier Ltd. All rights reserved.
doi:10.1016/j.jeurceramsoc.2008.10.009

cathodes. The electrolytes were pure gadolinia–ceria solid solution, CGO, and Bi_2O_3-doped CGO with improved densification, according to results described elsewhere.[8] The thermal expansion behaviour of these ceramics was measured by dilatometry and scanning electron microscopy; EDAX analysis was performed in cathode–electrolyte interfacial regions in order to characterize the obtained microstructures and to determine possible cation interdiffusion between the cathode and the electrolyte.

2. Experimental

2.1. Powder synthesis and compatibility studies

Ceramic powders of the composition $NdMn_{0.5}Me_{0.5}O_3$ (Me = Ni, Co) were prepared using the ethylene-glycol metal nitrate polymerized complex process[9] by mixing precursors of $Nd(NO_3)_3{\cdot}5H_2O$ (ventron, 99.9%), $Mn(NO_3)_2{\cdot}4H_2O$ (Merk, 99.0%), $Ni(NO_3)_2{\cdot}6H_2O$ (Sigma–Aldrich, 99.0%) and $Co(NO_3)_2{\cdot}6H_2O$ (Alfa Aesar, 98.0%) in appropriate stoichiometric ratios. The obtained powders were calcined at 650 °C for 6 h in air and wet-milled with ethanol for 2 h in an attrition ball milling using zirconia balls. These powders will be denoted in the following as NNiM and NCoM. More details of the powder preparation are given elsewhere.[10]

Ceria-based electrolyte powders, $Ce_{0.9}Gd_{0.1}O_{1.95}$, were processed by two alternative routes, one of which involves co-precipitation from aqueous nitrate solution, using ammonium hydroxide as precipitant agent (powders lately calcined at 600 °C for 2 h) and the other involved adding 1.0 wt% Bi_2O_3 as a sintering aid to a submicronic (400 nm mean particle size, according manufacturer) commercial $Ce_{0.9}Gd_{0.1}O_{1.95}$ powder (Rhodia GmbH, FRG). These powders will be denoted as CGO and CGO-Bi.[11]

X-ray powder diffraction (Siemens D-500, CuKα radiation) analysis was carried out for the reactivity studies. For this, equal amounts of the cathode and electrolyte powders were ground, pressed into pellets and then heat treated in air between 1350 and 1450 °C for 4 h and then annealed at 1000 °C for 100 h in air.

Finally, the shrinkage behaviour was characterized using a dilatometer Netzsch (model 407/E, Selb-Bayern Germany) and the coefficients of linear thermal expansion of the single ceramics were measured during the cooling cycle, once sintered at the corresponding temperature. Measurements were performed at a heating and cooling rate of 5 °C/min.

2.2. Semicell fabrication and characterization

Calcined and milled NNiM, NCoM and CGO powders were isostatically pressed at 200 MPa to prepare pairs of NNiM/CGO and NCoM/CGO, which were subsequently sintered at 1400 °C for 2 h. Pairs with $Ce_{0.9}Gd_{0.1}O_{1.95}$ + 1.0 wt% Bi_2O_3 (CGO-Bi) electrolytes (NNiM/CGO-Bi and NCoM/CGO-Bi) were also

Table 1
Physical parameters of the ceramic powders selected to produce cathode–electrolyte pairs.

Compositions	Calcination conditions	Mean particle size (TEM) (nm)	Mean agglomerate size (SEM) (μm)
$Ce_{0.9}Gd_{0.1}O_{1.95}$	600 °C/120 h	$20^{\pm10}$	0.5–1.7
$NdCo_{0.5}Mn_{0.5}O_3$	650 °C/6 h	$50^{\pm10}$	0.6–1.6
$NdNi_{0.5}Mn_{0.5}O_3$	650 °C/6 h	$45^{\pm10}$	0.5–1.5

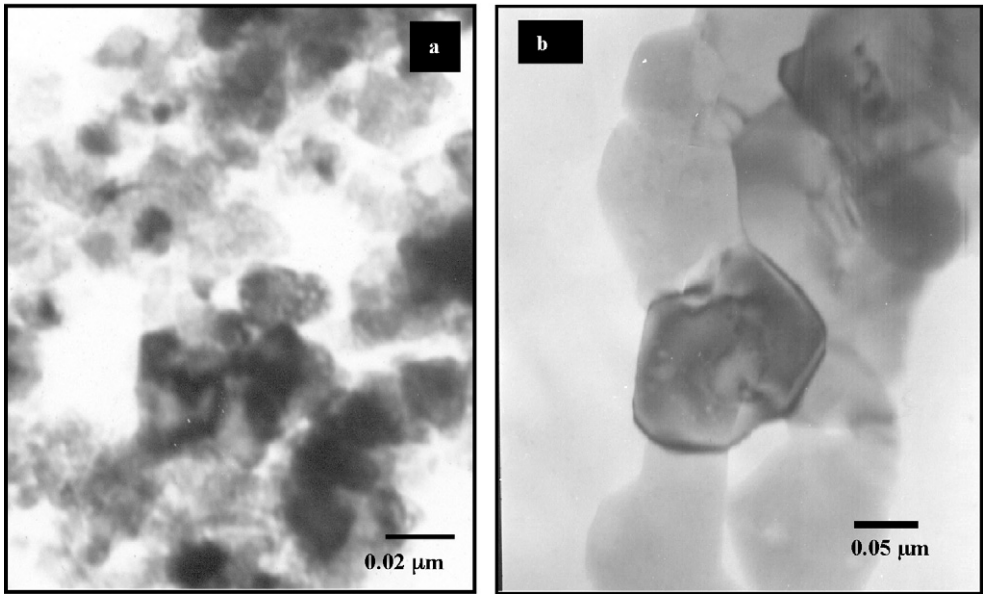

Fig. 1. TEM images of the synthesized and calcined powders: (a) $Ce_{0.9}Gd_{0.1}O_{1.95}$ prepared by the precipitation technique. (b) $Ce_{0.9}Gd_{0.1}O_{1.95}$ + Bi_2O_3, prepared from commercial powders.

prepared and sintered at 1350 °C for 2 h. The selected temperatures were based on the densification results and electrical properties previously obtained for both types of electrolyte and cathode.[10,11] The polished and fractured cross-sections were observed with scanning electron microscopy (SEM) in order to characterize the microstructure. Cation analysis was performed by EDAX in order to investigate their possible interdiffusion across the interface between the cathode and the electrolyte.

Table 2
Lattice parameters of electrodes and electrolytes.

Samples	Symmetry	*a* (nm) (±0.0001)	*b* (nm) (±0.0001)	*c* (nm) (±0.0001)	Vol. (nm^3)	*b*/*a*	Orth. Struct.
$NdNi_{0.5}Mn_{0.5}O_3$	Orthorhom.	0.5428	0.5560	0.7510	0.2267	1.024	O′-type
$NdCo_{0.5}Mn_{0.5}$ O_3	Orthorhom.	0.5433	0.5579	0.7527	0.2281	1.027	O′-type
CGO	Cubic	0.5415	–	–	0.1588	–	Fluorite-type
CGO-Bi	Cubic	0.5416			0.1589		Fluorite-type

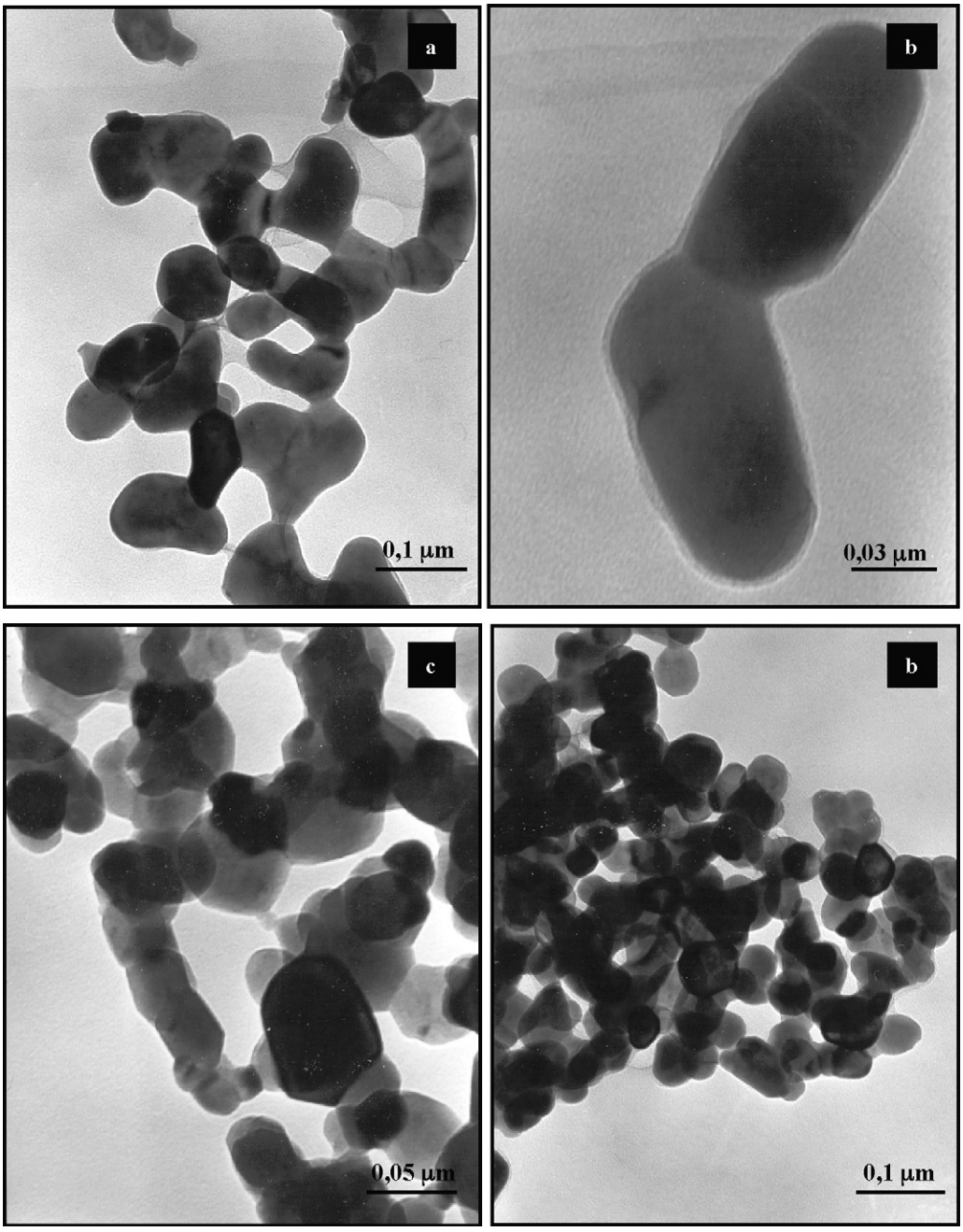

Fig. 2. TEM images of (a and b) $NdCo_{0.5}Mn_{0.5}O_3$ and (c and d) $NdNi_{0.5}Mn_{0.5}O_3$ prepared by the ethylene-glycol process.

3. Results and discussion

3.1. Powder characteristics

Table 1 shows the physical parameters of the ceramic powders selected to produce cathode–electrolyte pairs. TEM micrographs of the CGO, NNiM and NCoM calcined powders are shown in Figs. 1 and 2, respectively. All powders showed near spherical geometry and the particle size distribution was narrow. The average particle sizes of the manganite powders are similar in both cases for $NdMe_{0.5}Mn_{0.5}O_3$ (Me = Ni, Co) with values around 50 nm as can be determined by TEM (Fig. 2); the particle size is something lower for the case of NNiMn, probably due to its lower reactivity in comparison with that of NCoMn. The particles of doped ceria powders obtained via the chemical route are much smaller than those of commercial CGO. The average particle size of the commercial powder is ~400 nm (not represented), while the synthesized powder has fine particles with average size ~20 nm (Fig. 1).

The XRD patterns of the NMeM powders (not presented here) after calcining at 650 °C for 6 h, exhibit all the peaks corresponding to a well-crystallized perovskite phase with an orthorhombic Pbnm space group. In the case of both the CGO powders, the XRD pattern showed all the diffraction peaks associated with a pure fluorite structure; both the commercial CGO powder and co-precipitated one showed peaks rather broadened due to its extremely fine microcrystalline structure. Table 2 lists the lattice parameters of the electrolytes and cathodes.

The coefficients of thermal expansion (CTE), α, obtained from the slopes of the thermal expansion curves during cooling, between 1400 and 100 °C, are summarized in Table 3. For the sake of comparison, CTE values of some of the most commonly ceramic materials used as SOFC cathodes previously reported in the literature are included.

The thermal expansion coefficients of the cathodes vary widely, increasing in the sequence NCoM < CGO < NNiM. Although it is confirmed that a certain difference between

Table 3
Coefficients of thermal expansion of electrolytes (GDC-Bi and GDC) and doped manganites $NdMe_{0.5}Mn_{0.5}O_3$ (Me = Ni, Co) measured during cooling from 1400° to 100 °C.

Experimental results		Literature	
Compositions	α ($\times 10^6$ K^{-1})	Compositions	$\alpha \times 10^6$ (K^{-1})
CGO-1% Bi_2O_3	12.6	[7]$Nd_{0.95}MnO_3$	7.6
CGO	12.7	[7]$La_{0.95}MnO_3$	8.7
$NdCo_{0.5}Mn_{0.5}O_3$	12.0	[8]$La_{0.7}Ca_{0.3}CrO_{3-\square}$	11.1
$NdNi_{0.5}Mn_{0.5}O_3$	13.1	[9]$Sm_{0.6}Sr_{0.4}Co_{0.2}Fe_{0.8}O_3$	14.5

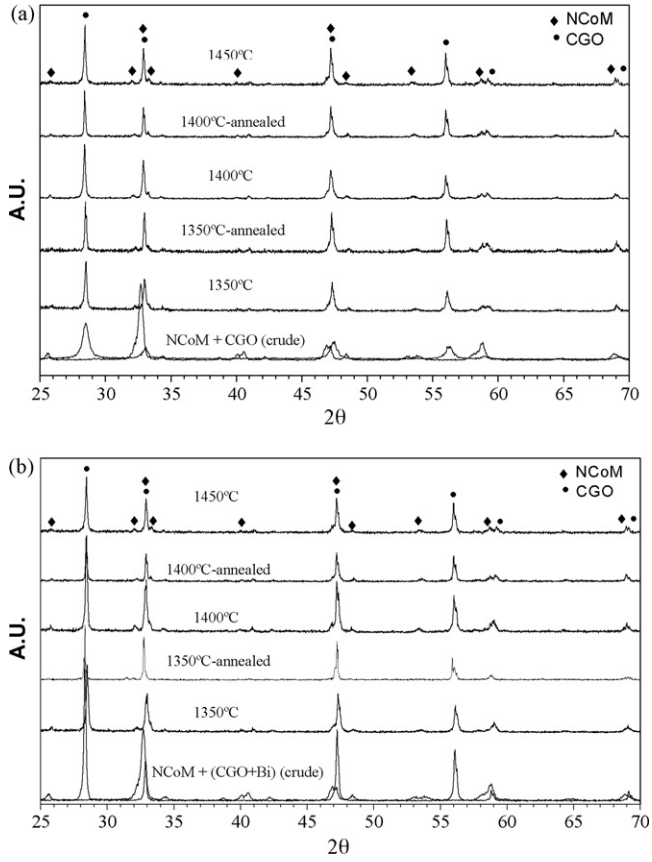

Fig. 3. XRD patterns of mixed powders fired between 1350 and 1450 °C for 4 h and after annealing in air at 1000 °C for 100 h: (a) $[NdCo_{0.5}Mn_{0.5}O_3] + [Ce_{0.9}Gd_{0.1}O_{1.95}]$ and (b) $[NdCo_{0.5}Mn_{0.5}O_3] + [Ce_{0.9}Gd_{0.1}O_{1.95}$ + 1% wt $Bi_2O_3]$.

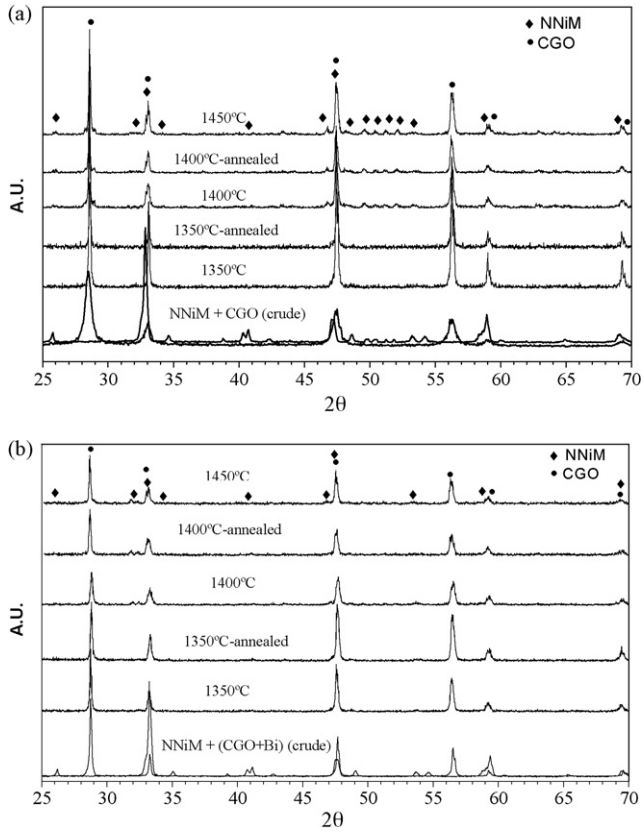

Fig. 4. XRD patterns of mixed powders fired between 1350 and 1450 °C for 4 h and after annealing in air at 1000 °C for 100 h: (a) $[NdNi_{0.5}Mn_{0.5}O_3] + [Ce_{0.9}Gd_{0.1}O_{1.95}]$ and (b) $[NdNi_{0.5}Mn_{0.5}O_3] + [Ce_{0.9}Gd_{0.1}O_{1.95}$ + 1% wt $Bi_2O_3]$.

the CTE of electrolytes ($\alpha = \sim 12.6 \times 10^{-6}\,K^{-1}$) and selected cathodes ($\alpha = 12–13 \times 10^{-6}\,K^{-1}$) exists, the differences are smaller than those reported in other types of ceramic materials used as cathodes, such as some manganites[12] ($\alpha = \sim 7.5–8.5 \times 10^{-6}\,K^{-1}$), chromites[13] ($\alpha = \sim 11 \times 10^{-6}\,K^{-1}$) or ferrites[14] ($\alpha = \sim 14 \times 10^{-6}\,K^{-1}$). As a result, although these materials have excellent electrical properties, they cannot be used with electrolytes based on ceria, since the great thermal mismatch would produce cracks or even the failure of the cell. It is noted that a small amount of bismuth oxide on the ceria gadolinia solid solution does not affect the thermal expansion behaviour of the ceramic material.

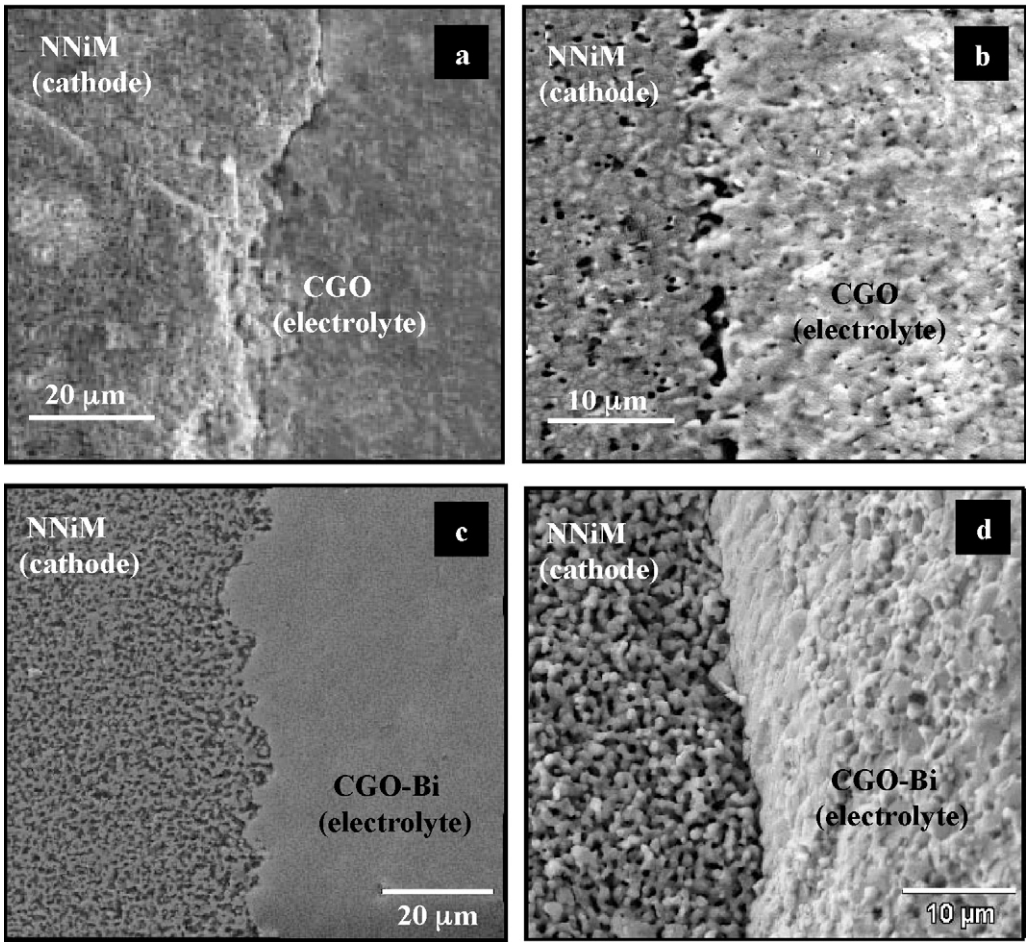

Fig. 5. (a and c) Polished surface and (b and d) fracture surface of cross-sectional views of typical electrolytes cosintered with cathodes $NdNi_{0.5}Mn_{0.5}O_3$, to form pairs (a and b) NNiM/CGO (1400 °C–2 h) and (c and d) NNiM/CGO-Bi (1350 °C–2 h). Temperatures correspond to the maximum density for both electrolytes.

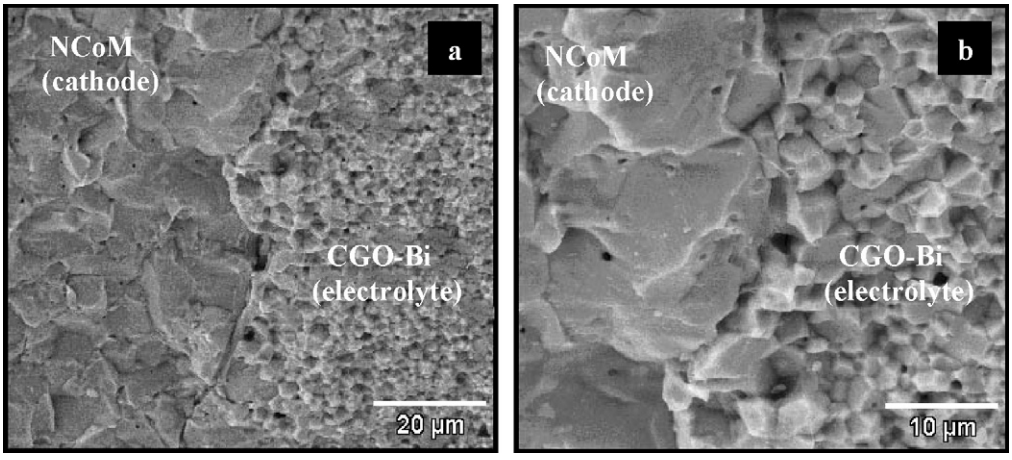

Fig. 6. (a) Polished surface and (b) fracture surface of cross-sectional views of an electrolyte CGO-Bi cosintered at 1350 °C-2 h with a $NdCo_{0.5}Mn_{0.5}O_3$ cathode.

3.2. Chemical compatibility

In general, an important problem in the use of perovskite materials for SOFC applications is their reactivity with most electrolyte materials, which leads to the formation of undesirable new phases along the cathode–electrolyte interface that can affect the electrical conductivity.[15] For this reason, and in order to study the possible reactions between the NMeM and CGO phases, powder mixtures were prepared and treated at several high temperatures for 4 h and subsequently annealed in air at 1000 °C during long times (4–100 h), as was mentioned above.

Fig. 3(a) and (b) displays the XRD patterns of the NCoM + CGO and NCoM + (CGO + Bi) mixtures, respectively, before and after heat-treatment, and Fig. 4(a) and (b) displays the XRD patterns of the NNiM + CGO and NNiM + (CGO + Bi) pairs, respectively. In all cases, it is observed that the initial phases maintain their crystalline structures without degradation at all the studied temperatures and times. According to the obtained results, the perovskite systems seem to be compatible with the ceria electrolyte, even in the most severe conditions (i.e. 1450 °C), at least at the level of observation corresponding to the sensitivity of the XRD analyses. Peaks corresponding to the 44–55° range, which are apparent in Fig. 4(a), pattern 1450 °C, are less conspicuous in Fig. 4(b), but a detailed analysis of this pattern showed its presence. These peaks correspond to the perovskite structure, and thus were indexed for both pattern types.

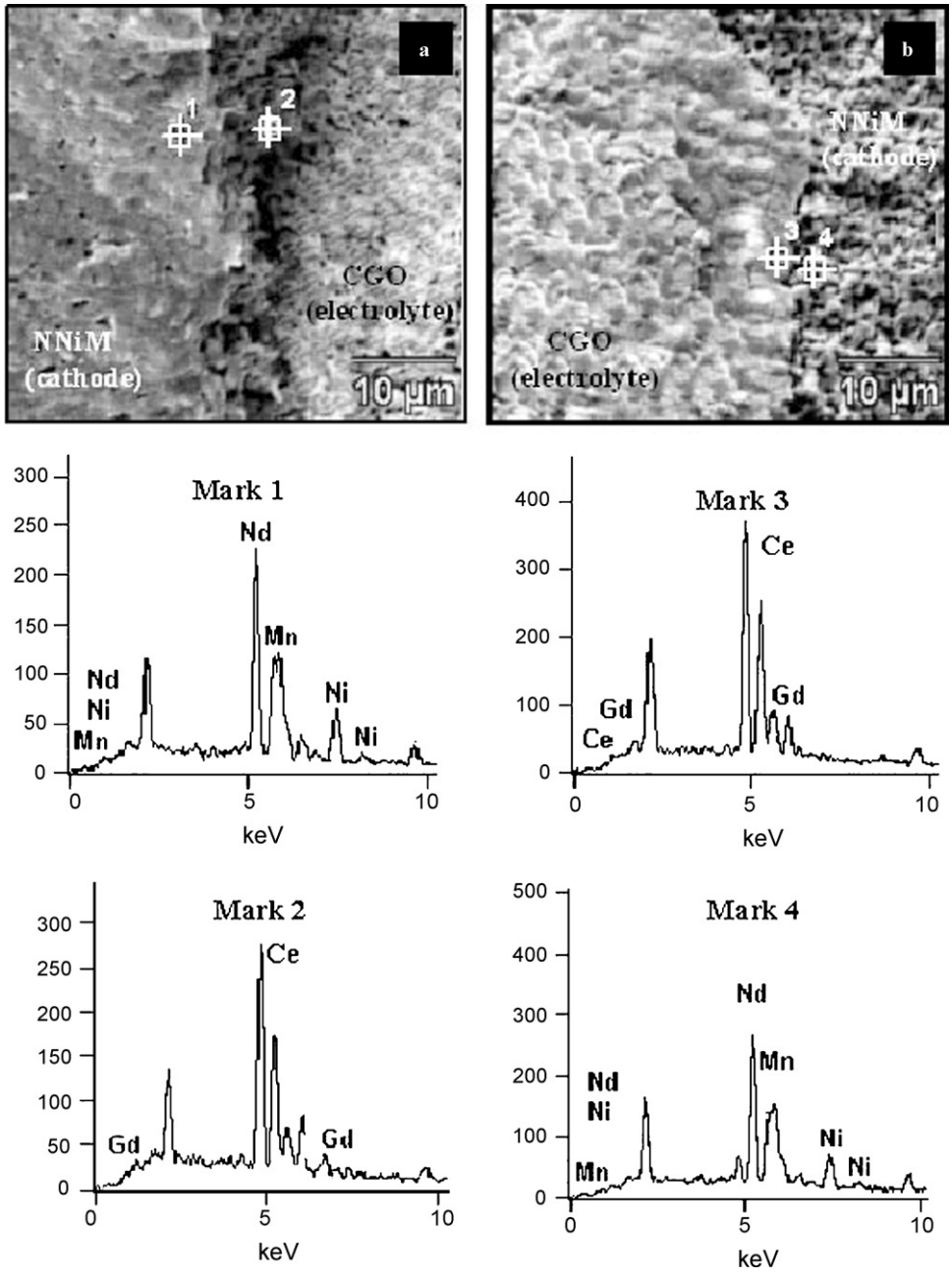

Fig. 7. EDAX analysis on interface: (a) NNiM/CGO and (b) NNiM/CGO-Bi cosintered at 1400 and 1350 °C, respectively. Temperatures correspond to the maximum density for both electrolytes.

3.3. Interface microstructural characterization

In order to assure that the two layers bonded perfectly and formed a well-defined interface without second phases, and that cation diffusion does not take place through the interfacial region, cosintered sandwiches were characterized by scanning electron microscopy.

Fig. 5 shows SEM images of fractured and polished cross-sectional surfaces corresponding to $NdNi_{0.5}Mn_{0.5}O_3$ cathodes cosintered with $Ce_{0.9}Gd_{0.1}O_{1.95}$ or $Ce_{0.9}Gd_{0.1}O_{1.95}$ + 1.0 wt% Bi_2O_3 electrolytes.

Both applied thermal treatments (1400 and 1350 °C during 2 h, corresponding to temperatures for which ceria electrolytes attain the better densification) resulted in a good connectivity between the cathode and the electrolyte layers, with a well-defined interface and without the apparent presence of any new secondary phases, which seems to correlate with the XRD results. Furthermore, the good adhesion between the layers of the pairs and the absence of structural defects (e.g. cracks or delaminations) confirm a good matching of the coefficients of thermal expansion during the cosintering process. Both thermal treatments resulted in electrolytes with very homogenous microstructures, with a submicronic average grain size (~0.8 μm) and high sintered density (>94% theoretical XRD density, D_{th}), according to data for electrolyte layer for which the cathode layer has been pulled out. This apparent density is enough to ensure a good cell operation. In the case of the electrolyte doped with a small amount of bismuth oxide, the density is somewhat higher (97% vs. 95% D_{th}).

The cathode microstructure obtained at a lower sintering temperature (1350 °C) shows in a uniform structure with a small grain size (0.7–1 μm) and a highly interconnected porosity of ~0.5 μm, while the higher thermal treatment temperature (1400 °C) of the cathode, eliminated part of its porosity.

In the case of the formation of the mixtures with cobalt-doped manganite, cathode microstructures are similar for both sintering temperatures (1350 and 1400 °C). Here, only the cross-sectional view corresponding to the pair prepared with the electrolyte doped with bismuth oxide (NCoM/CGO-Bi) and cosintered at lower temperature (1350 °C for 2 h) is shown in Fig. 6. It is observed that layers remain with a good connectivity and the interface is free of cracks, as can be predicted from the data collected measuring the coefficients of thermal expansion. Nevertheless, these manganite cathodes are very heterogeneous and present an exaggerate grain growth (~5–20 μm vs. ~0.8 μm for CGO ceramics) in the temperature range 1350–1400 °C. This behaviour could deteriorate the mechanical properties of the final product, resulting in a mechanically weak cell. Thus, they are not suitable for use as cathodes in SOFC applications, where the thermal treatments are equal to or exceed 1350 °C. For this reason, EDAX analysis was performed only on the NNiM/CGO-Bi interface.

In order to confirm the absence of cation migration across the interfacial region, EDAX analyses on located regions were carried out (Fig. 7). EDAX spectra show that in the cathode region located near the interface, a number of peaks appear at the positions expected for a system that contains Nd, Ni and Mn elements. That is, there is no cerium or gadolinium diffusion from the electrolyte into the cathode. Similarly, neodymium, nickel or manganese diffusion was not detected at the electrolyte surface even close to the electrode.

4. Conclusions

Neodymium-based perovskites, $NdMn_{0.5}Me_{0.5}O_3$, are chemically compatible with the fluorite type ceramic $Ce_{0.9}Gd_{0.1}O_{1.95}$, i.e. no reaction products have been observed after heat treatments as high as 1450 °C. Therefore, it is possible to co-sinter single semicells of NNiM/CGO (or NNiM/CGO-Bi) and NCoM/CGO (or NCoM/CGO-Bi), without the appearance of new phases in the boundary between electrode and electrolyte.

The pairs constituted from nickel-doped manganite as cathode material present (when are deposited on both electrolytes) well-defined and crack-free interfaces, as expected from the study of the coefficients of thermal expansion. Furthermore, these nickel-doped manganites have a good microstructure (no exaggerated grain growth or pore closure is observed) at thermal treatment temperatures between 1350 and 1400 °C. Thus, these materials should perform excellently as cathodes for the CGO-based SOFCs, where thermal treatment temperatures up to 1400 °C are required.

Acknowledgements

Financial support from the CICYT MAT 2003-01163.Project and a grant from the Autonomous Community of Madrid are gratefully acknowledged.

References

1. Yamamoto, O., Takeda, Y., Kanno, R. and Noda, M., Perovskite-type oxides as oxygen electrodes for high-temperature oxide fuel-cells. *Solid State Ionics*, 1987, **22**, 241.
2. Adler, S. B., Factors governing oxygen reduction in solid oxide fuel cell cathodes. *Chemical Reviews*, 2004, **104**, 4791.
3. Mobius, H. H., On the history of solid electrolyte fuel cells. *Journal of Solid State Electrochemistry*, 1997, **1**, 2.
4. Lau, S. K. and Singhal, S. C., Potential electrode/electrolyte interactions in solid oxide fuel cells. *Corrosion*, 1985, **85**, 345, Boston, MS, USA.
5. Taimatsu, H., Wada, K., Kaneko, H. and Yamamura, H., Mechanism of reaction between lanthanum manganite and yttria-stabilized zirconia. *Journal of the American Ceramic Society*, 1992, **75**, 401.
6. Yokokawa, H., Saka, N., Kawada, T. and Dokiya, M., Thermodynamic analysis on interface between perovskite electrode and YSZ electrolyte. *Solid State Ionics*, 1990, **40–41**, 398.
7. (a) Kostogloudis, G. C. and Ftikos, Ch., Effect of Sr-doping on the structural and electrical properties of gadolinium manganite oxide. *Journal of Material Science*, 1999, **34**, 2169;
(b) Kostogloudis, G. C. and Ftikos, Ch., Characterization of $Nd_{1-x}Sr_xMnO_{3\pm\delta}$ SOFC cathode materials. *Journal of European Ceramic Society*, 1999, **19**(4), 497–505.
8. Gil, V., Tartaj, J., Moure, C. and Durán, P., Sintering, microstructural development, and electrical properties of gadolinia-doped ceria electrolyte with bismuth oxide as a sintering aid. *Journal of the European Ceramic Society*, 2006, **26**, 3161–3171.
9. Duran, P., Tartaj, J., Rubio, F., Peña, O. and Moure, C., Preparation and powder characterization of spinel-type $Co_xNiMn_{2-x}O_4$ ($0.2 < x < 1.8$) by

the ethylene glycol–metal nitrate polymerized complex process. *Journal of European Ceramic Society*, 2004, **24**, 3035.

10. Moure, C., Gil, V., Tartaj, J., Pena, O. and Durán, P., Powder processing, crystalline structure, sintering, and electrical properties of $NdM_{0.5}Mn_{0.5}O_3$ (M = Ni, Co, Cu) manganites. *Journal of European Ceramic Society*, 2005, **25**, 2661.
11. Gil, V., Moure, C., Durán, P. and Tartaj, J., Low-temperature Densification and grain growth of Bi_2O_3-doped-ceria gadolinia ceramics. *Solid State Ionics*, 2007, **178**, 359.
12. Wandekar, R. V., Wani, B. N. and Bharadwaj, S. r., High temperature thermal expansion and electrical conductivity of $Ln_{0.95}MnO_{3+\delta}$ (Ln = La, Nd or Gd). *Journal of Alloys and Compounds*, 2007, **433**, 84.
13. Zhou, X. and Ma, J., Preparation and properties of ceramic interconnecting materials, $La_{0.7}Ca_{0.3}CrO_{3-\square}$ doped with GDC for IT-SOFCs. *Journal of Power Sources*, 2006, **162**, 279.
14. Xu, Q., Huang, D. P., Chen, W. and Wang, B., Structure, electrical conducting and thermal expansion properties of $Ln_{0.6}Sr_{0.4}Co_{0.2}Fe_{0.8}O_3$ (Ln = La, Pr, Nd, Sm) perovskite-type complex oxides. *Journal of Alloys and Compounds*, 2007, **429**, 34.
15. Richland, W. A., *Chemical Interactions Between Interconnect and Electrode Materials During Sintering in Solid Oxide Fuel Cells, Alternative Electrodes and Interconnections for Solid Oxide Fuel Cells*. Laboratories Pacific Northwest Ed., 1993, p. 632–640.